U.S. Department of Energy
Energy Efficiency
and Renewable Energy
Bringing you a prosperous future where energy
is clean, abundant, reliable, and affordable

Idaho National Laboratory

Key Issues Regarding Electrolytes at Interfacial Regions
(subtask "low temperature performance")

Kevin L Gering, PhD

DOE-EERE Merit Review Meeting
May 19, 2009 (Arlington (Crystal City), VA)

Project ID:
esp_05_gering

This presentation does not contain any proprietary, confidential, or otherwise restricted information.

Idaho National Laboratory
International Nuclear Leadership for the 21st Century

Overview

Timeline	Barriers
Project Start: Oct. 2003 Project End: Sept. 2009 Percent Complete*: 90% * for subtask "low temperature performance". Modeling support will continue for key issues within DOE-ABRT.	Many Li-ion battery systems undergo a marked decrease in performance at low temperatures. Such performance limitations prevent Li-ion technologies from being fully deployed in HEV/PHEV applications for cold climate scenarios. An essential step in mitigating such barriers is to better understand plausible root causes tied to the interfacial behavior of electrolytes that would exist given the physics and thermodynamics of interfacial regions in the cell environment.
Budget	**Partners**

Funding Received:
  FY 08: $230K
  FY 09: $70K (task completion)
	INL has collaborated with ANL regarding low-temperature performance (D. Dees, A. Jansen), and with ARL in earlier years (R. Jow).
	
	INL has also utilized its modeling capabilities to collaborate with the Private Sector (Air Products and Chemicals, Inc., EIC Labs, Battery Design Studio), and has received numerous other inquiries.

Idaho National Laboratory

Scope

Objectives

To gain further understanding of how performance of Li-ion batteries depends on interfacial behavior of electrolytes at open circuit voltage (OCV) and cycling conditions, particularly at low temperatures. This is done to identify plausible mechanisms for performance limitations tied to the battery electrolyte, leading to a more informed mitigation plan based in part on alternative electrode materials and electrolyte components .

This concurs with the stated Programmatic Strategy of the Electrochemical Energy Storage Technical Team Technology Development Roadmap, section 3.4.2.2 *Enhance Low-Temperature Performance.*
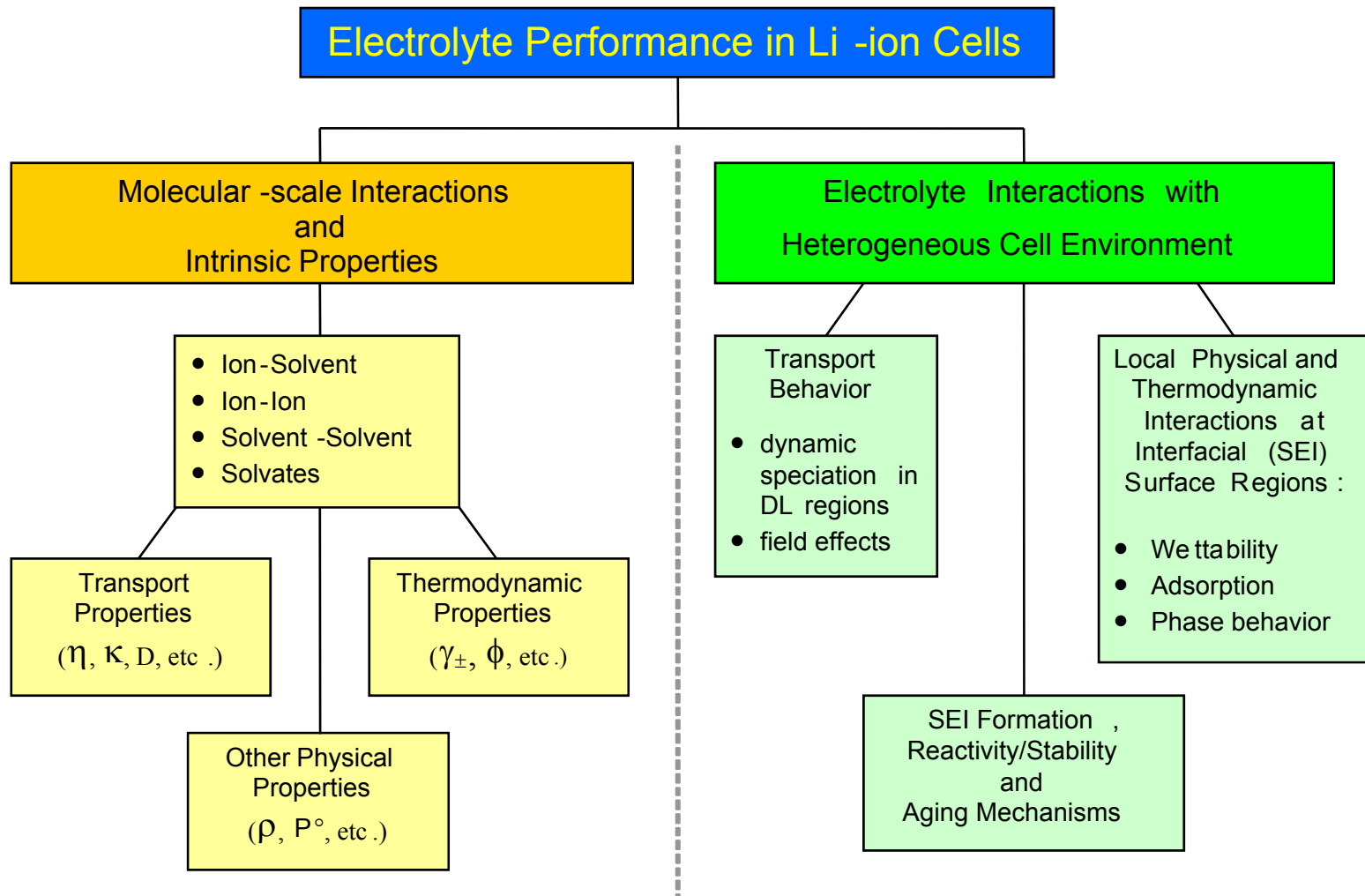
Approach

Models: This work is based on modeling capabilities developed at the INL under the DOE-ABRT program (previously ATD): Advanced Electrolyte Model (AEM), and a new cell performance model that examines pertinent issues of kinetic performance, denoted θ-BV.

Data: Diagnostic testing provides supporting data toward model validation and identifying probable origins for performance trends.

Milestones

(refer to Technical Accomplishments)

There are Numerous Interactions Involving Electrolytes in Li-ion Cells

Electrolyte Modeling Overview

The shown elements are the foundation for advanced characterization, screening and optimization for numerous applications.

Core database covers:
- *15 solvents*
- *6 salts*

viable for Li-ion systems.

The model also covers multi-solvent and mixed salt electrolytes.

Transport Properties
(molecular basis)

- Viscosity: η
- Conductivity: κ
- Diffusivity: D
- Transference Number : t_+ etc.

Key properties are generally predicted to within 5-10 % of experimental values over wide ranges of T and composition.

Many predictions reach agreement to $\leq 5\%$.

Ion Solvation Quantities
(via chemical physics equation of state)

- HS and effective transport diameters of cation and anion as f(comp., T):

$$\sigma_j^{HS}, \sigma_j^{eff}$$

- Solvation numbers: n_{s+}, n_{s-}
- Solvent residence times: τ_+, τ_-

Thermodynamic Properties
(Associative MSA basis)

- Activity Coefficient: $\gamma_\pm$
- Osmotic Coefficient: ϕ_m
- Ion Pair Formation (CIP, SSIP)
- Triple Ion Formation
- Onset of solid solvates

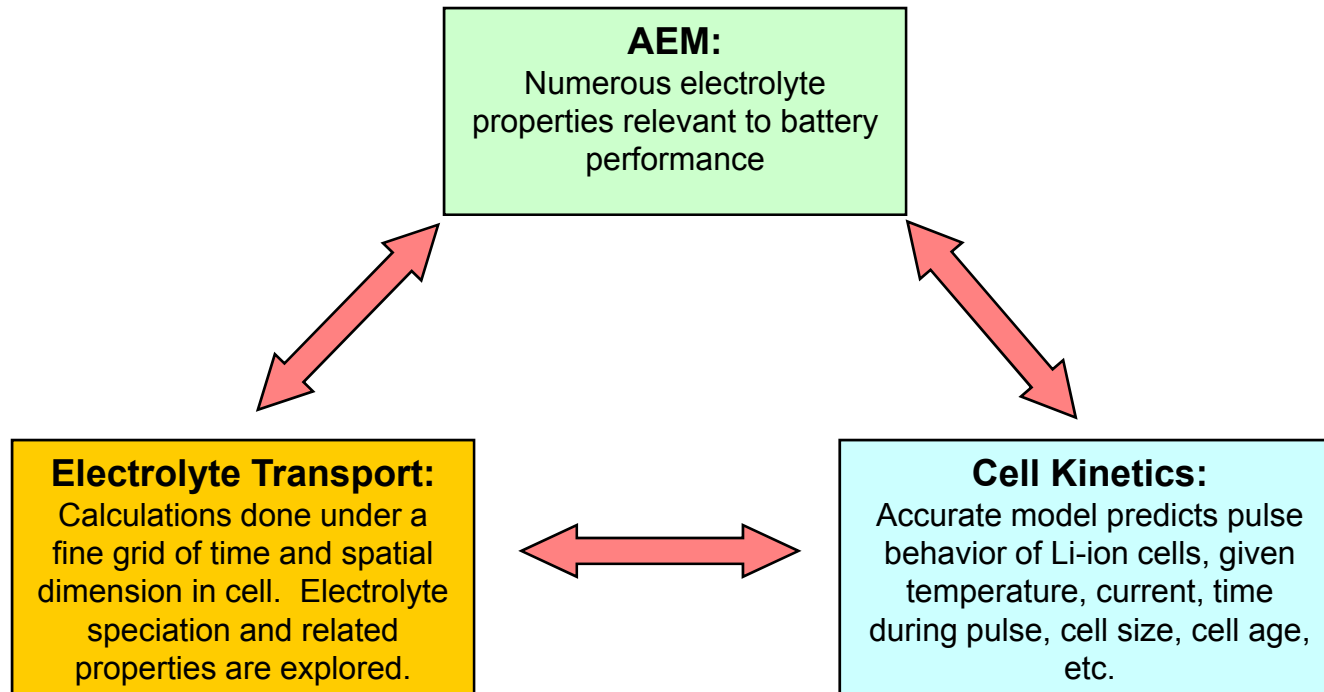## Energy, Dielectric Quantities
(Molecular, Thermodynamic bases)

- Gibbs free energy of ion solvation
- Solvent-to-ion Binding Energy for cation and anion
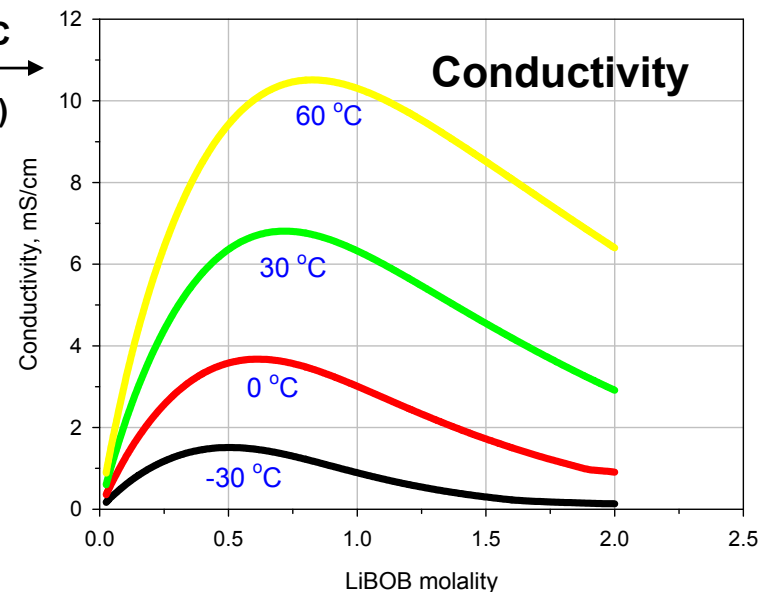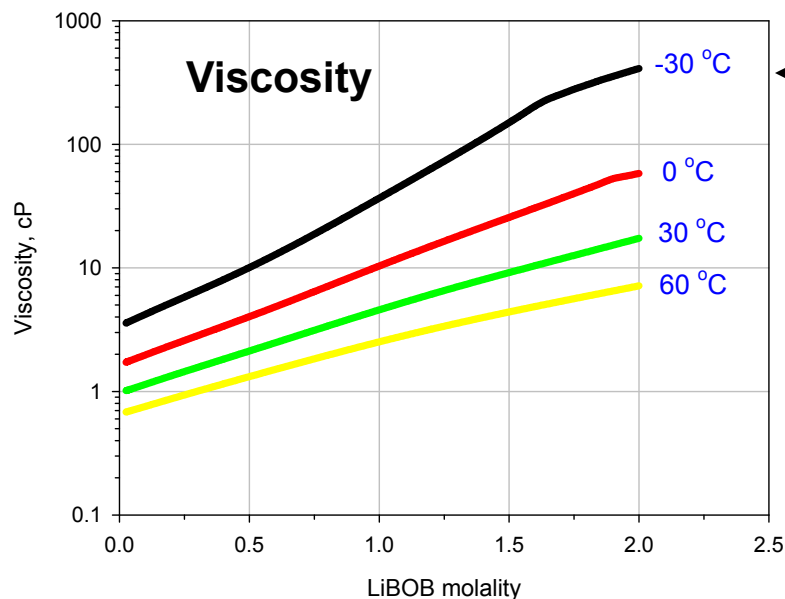- Relative enthalpy
- Dielectric Depression

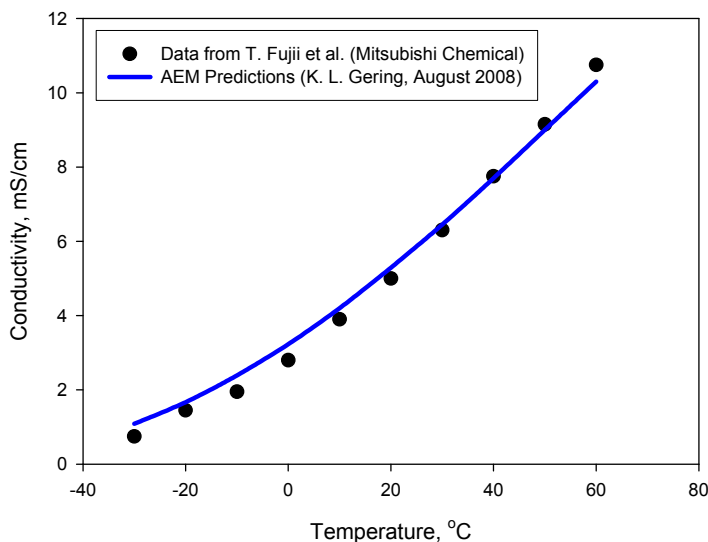# Overall Modeling Approach

Technical Accomplishments in 2008

1. The system EC-EMC-LiBOB was modeled over salt concentration and temperature and the suite of transport properties was forwarded to ANL.

2. The infrastructure for applying the AEM to cell-level transport modeling (e.g., double layer (DL) regions) was improved and expanded.

3. Simulations covering low temperature cell discharge showed that electrolyte speciation in cathode DL can lead to lower rates of charge transfer, while ion enrichment within the anode side DL can result in significant local worsening of transport properties (higher viscosity, lower conductivity and diffusivity).

4. A new kinetics model coupled with various diagnostic testing suggests that apparent kinetic limitations at low temperatures are actually governed by thermodynamically-driven mass transport limitations involving electrolyte solvent located at/near interfacial regions. A feature of the model is a modified form of the Butler-Volmer expression that accounts for the extent of surface availability in Li-ion cells, a necessary element given heterogeneous electrodes.

Idaho National Laboratory

EC-EMC (3:7) + LiBOB: selected AEM results

Viscosity — EC-EMC at (3:7, wt) — **Conductivity**

Conductivity of EC-EMC (3:7 vol.) + 0.85 M LiBOB

Model Validation

Data from T. Fujii et al. (Mitsubishi Chemical)
AEM Predictions (K. L. Gering, August 2008)

Modeling of this system was requested by Dennis Dees (ANL)

Utilizing the AEM as a Basis for Transport Modeling of Electrolyte Systems

Transport Modeling of Electrolytes

The AEM accounts for:

- Continuity expressions for all mobile species in a given electrolyte (single cations and anions, solvent, ion pairs, and triple ions (ABA,BAB)) over (x,t).

- Diffusion of all electrolyte species,

- Diffusion potential,

- The effects of ion solvation on solvent co-transport, and how this changes with species velocities,

- Explicit consideration of intrinsic lithium desolvation kinetics,

- Electrolyte properties over (x,t), including conditions of non-electroneutrality.

- Limiting packing fractions of electrolyte species,

- Considers a fine matrix of spatial dimension in x versus pulse time,

- Calculates current, resistance, net charge delivered, etc. over (x,t).

- Pulse type: –   constant potential or constant current
  - charge or discharge
  - duration and magnitude.
- *And More*

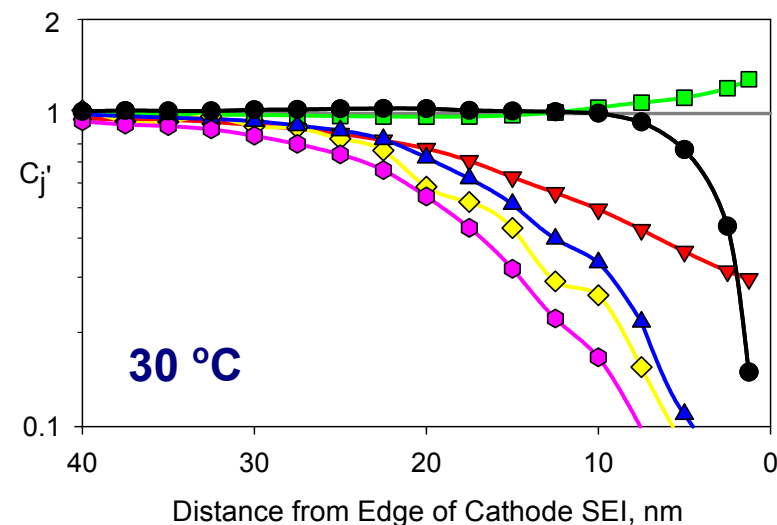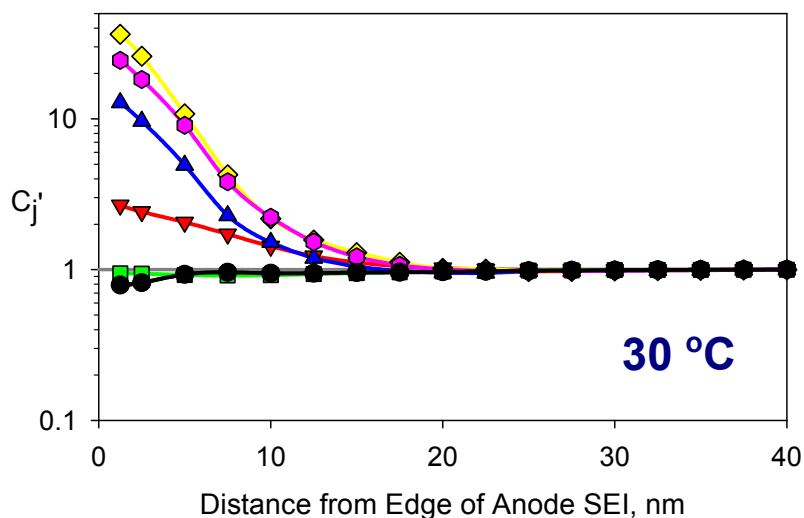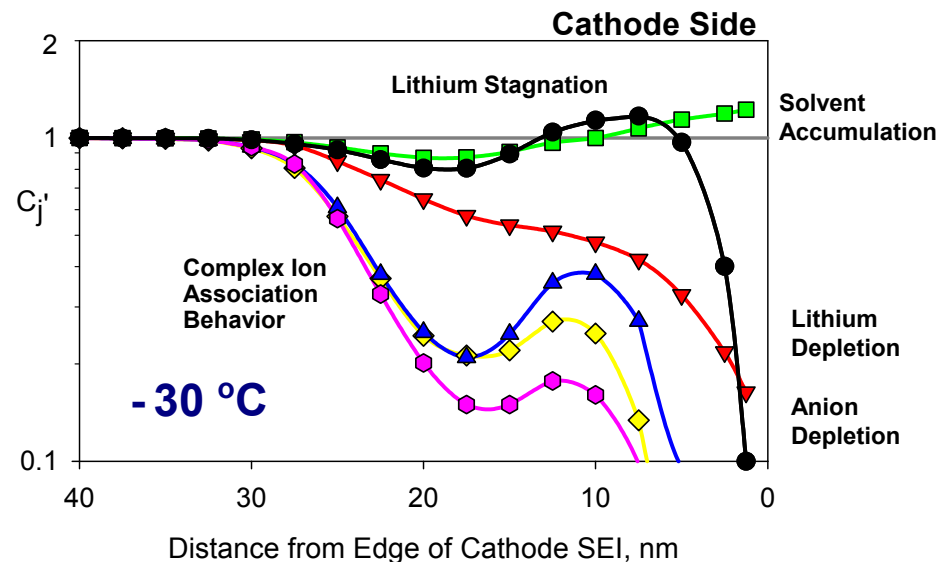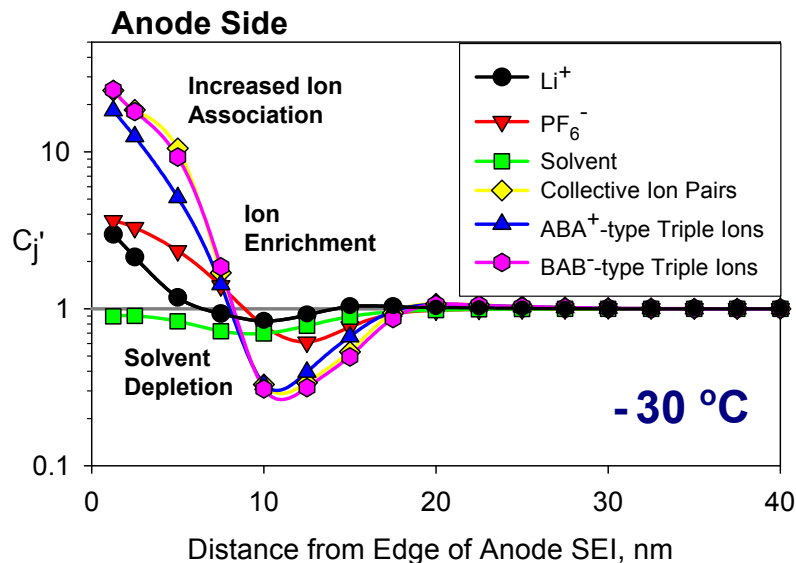# Sample Output for Transport Calculations

Conditions:

- ➢ Electrolyte: EC:EMC (3:7, vol.) + 1.2M $LiPF_6$
- ➢ Constant-current Discharge Pulse at 0.2 mA/cm^2
- ➢ Temperatures: -30 and 30 °C
- ➢ Pulse Time: 1.25 second, using 0.025s time steps
- ➢ Spatial grid: 2.5 nm step size in DL regions; larger in separator.
- ➢ Output for DL regions represented as

  - ▪ Spatially-dependent dimensionless concentrations of electrolyte species, normalized with time-zero values, and

  - ▪ Spatially-dependent transport properties.

Other results were obtained for electrolytes containing $LiBF_4$ and LiBOB, but were not included for sake of brevity. PI can discuss at poster session.

Idaho National Laboratory

Concentration Profiles (*normalized to time zero values*)
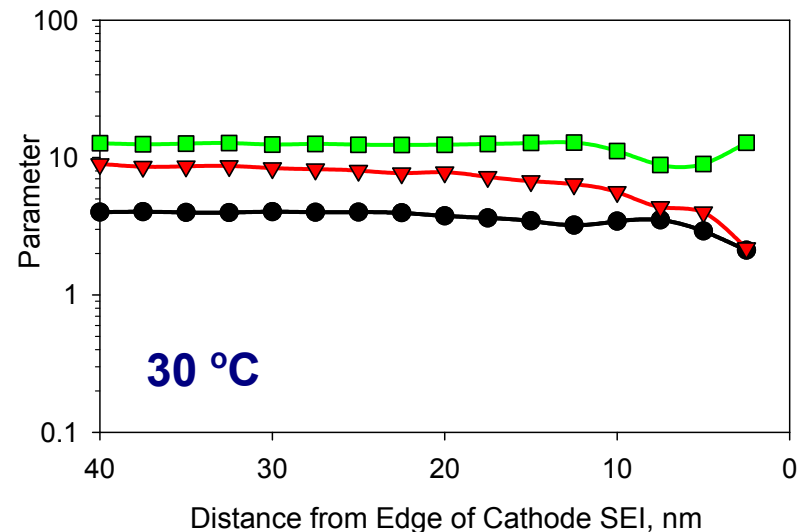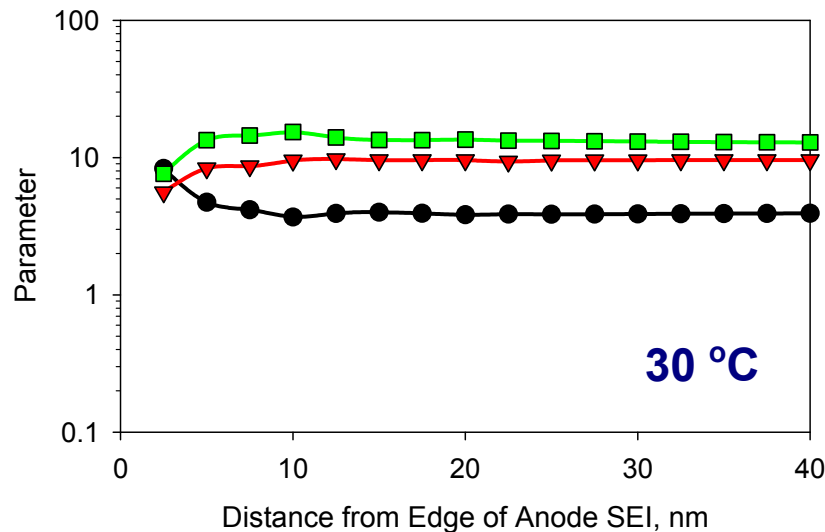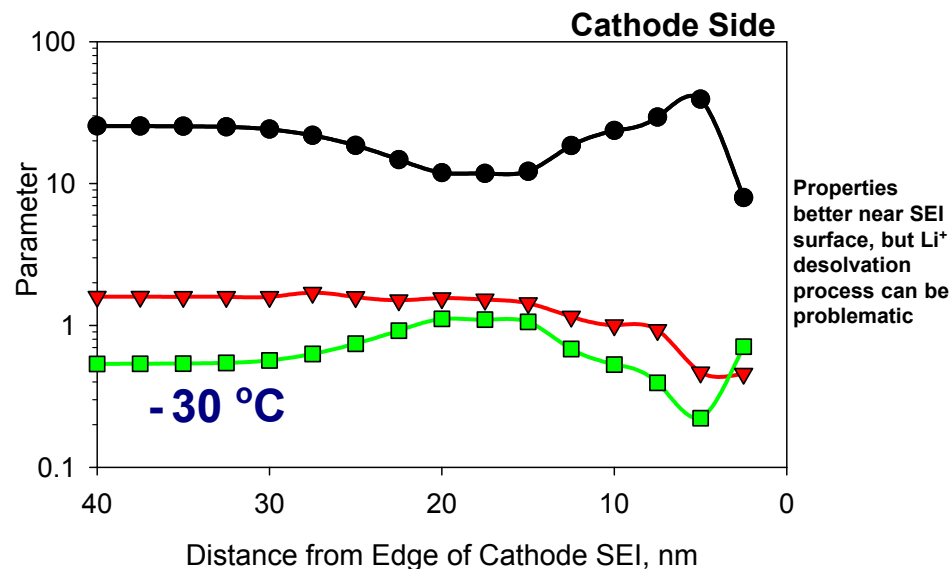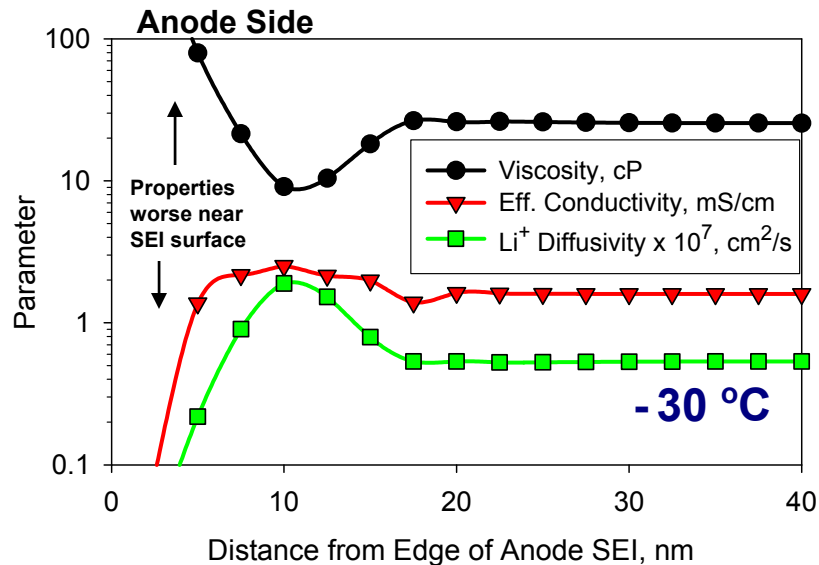# After 1.25-second Constant Current Discharge Pulse (0.2 mA/cm^2)

Results for Gen2 Chemistry, Electrolyte = EC:EMC (3:7) + 1.2M LiPF$_6$

Transport Property Profiles

After 1.25-second Constant Current Discharge Pulse (0.2 mA/cm^2)

Results for Gen2 Chemistry, Electrolyte = EC:EMC (3:7) + 1.2M LiPF$_6$

Cell Kinetics Study: Data and Model Development
What really affects the rate of charge transfer at low T?

(selected material presented at the 214th Meeting of the Electrochemical Society, abstract 1288, October 17, 2008)

Idaho National Laboratory

Cells and Test Conditions: Kinetics Study

Gen2 Cell Chemistry and Pulse Conditions:

Cathode: $LiNi_{0.8}Co_{0.15}Al_{0.05}O_2$ (35 μm laminate)

Anode: MAG-10 (35 μm)

Electrolyte: EC-EMC (3:7, mass) + 1.2M $LiPF_6$

Separator: Celgard 2300 series

Configuration: 18650

Electrode Area: 846.3 cm^2

SOC for all pulses: 60% (3.725V)

Pulse Duration (discharge)*: 10 s

Rest between pulses: 1hr

Four cells were tested having either 16-20% or 50-55% power fade.

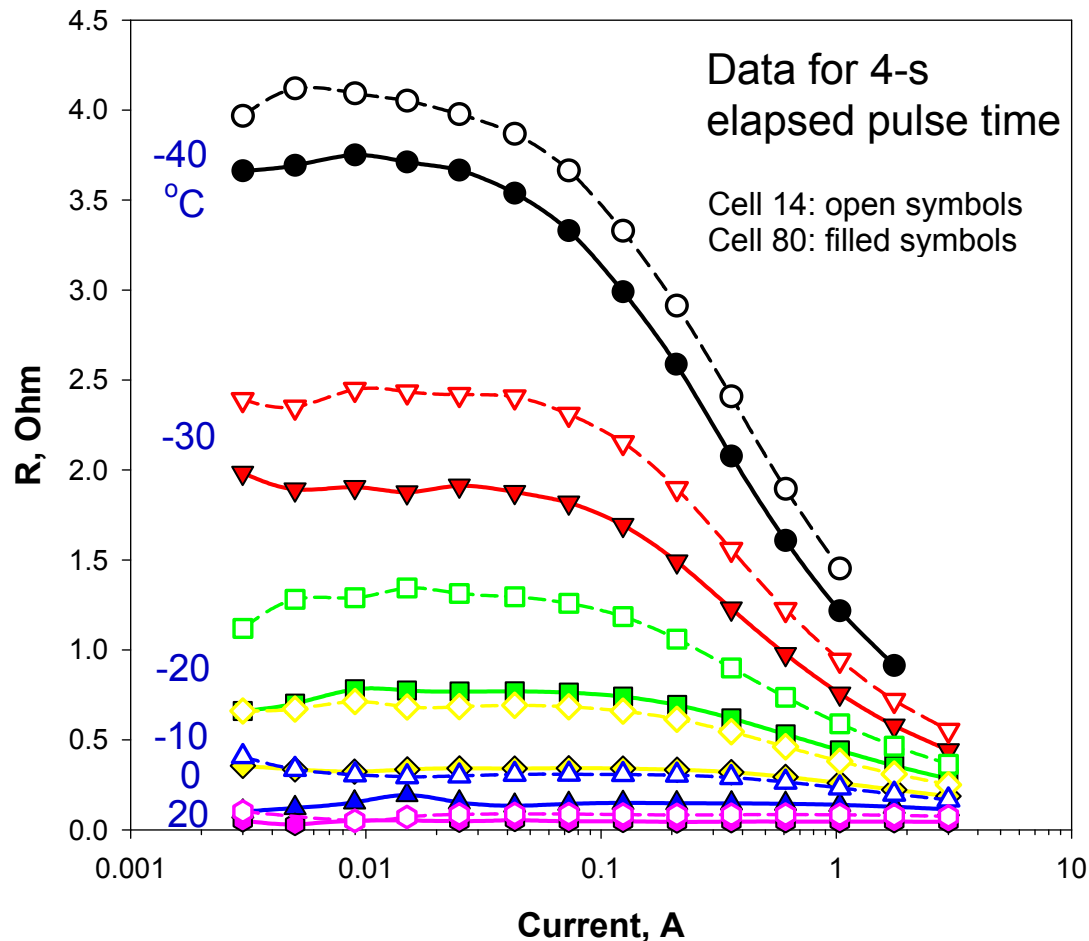* Charge pulse study was also performed, but results not shown herein.

It is assumed Joule heating and concentration overpotential are minor or negligible effects for short pulses up until the highest currents are reached.

Cell Behavior under Short Discharge Pulses

Cells 14 and 80 (Gen2 18650) discharge pulse impedance

(one hour rest between each constant-current pulse)

Cell 14: ≈ 50-55% Power Fade
Cell 80: ≈ 16-20% Power Fade

Data for 4-s
elapsed pulse time

Cell 14: open symbols
Cell 80: filled symbols

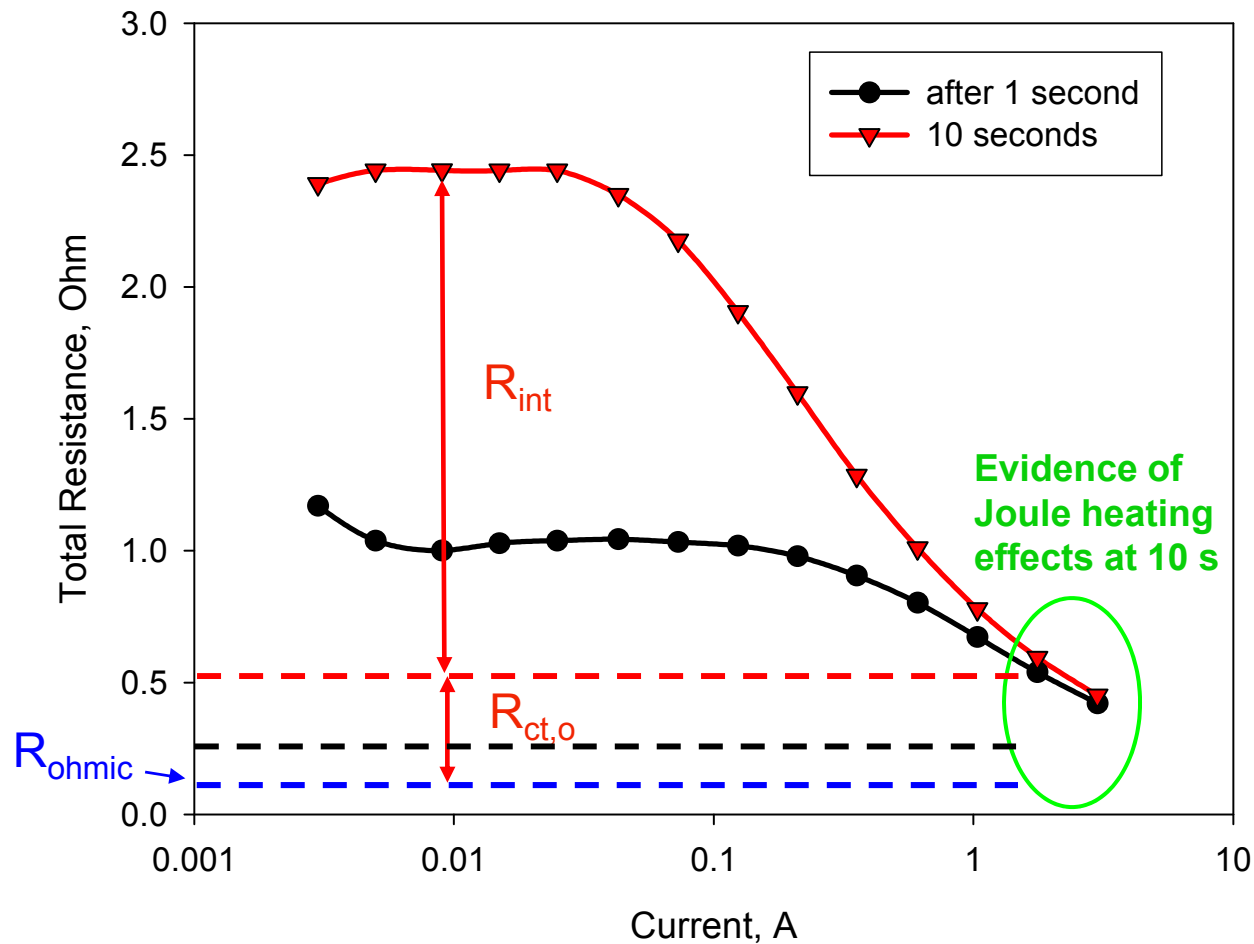There is a strong dependence of impedance on temperature and current.

Interfacial contributions to R dominate at low current but then rapidly diminish with increased current.

The effect of cell aging and pulse duration is markedly reduced at higher currents, where the curves tend to converge for a given T.

Collectively, this indicates an effective net reduction of interfacial impedance, but at the cost of power loss. What is the mechanism for this reduced interfacial impedance regarding SEI films?

Key Impedance Terms

Cell 80, -30 ^{o}C, constant-current discharge pulses

θ-BV Theoretical Development

θ-modified Butler-Volmer expression (ohmic corrected)

$$i = i_o \left[\exp\left(\frac{\theta_{eff}\ \alpha_{a,o}\ F\left(\eta - \eta_{ohm}\right)}{RT} \right) - \exp\left(\frac{-\theta_{eff}\ \alpha_{c,o}\ F\left(\eta - \eta_{ohm}\right)}{RT} \right) \right]$$

where θ_{eff} is the average effective fraction of electrode surface availability for charge transfer, as f(T, aging).

Effective transfer coefficients: $\qquad \alpha_a = \theta_{eff}\ \alpha_{a,o} \quad$ and $\quad \alpha_c = \theta_{eff}\ \alpha_{c,o}$

Some investigators* have reported effective transfer coefficients well below the theoretical value of 0.5, and have attributed such values to reduced availability of the electrode surface due to fouling or occlusion. In Li-ion cells, surface occlusion observed over T would be mostly tied to electrolyte behavior.

* e.g., J. Wang and J. Farrell, *J. Appl. Electrochemistry*, vol. 35, pp 243-248, 2005; M. H. P. Santana, L. A. De Faria, J. F. C. Boodts, *Electrochem. Acta*, vol. 50, pp 2017-2027, 2005.

θ-BV Theoretical Development, p2

Apparent Charge Transfer Resistance (θ_{eff} basis):

$$R_{ct,app} = \left(\frac{\eta - \eta_{ohm}}{i A_e}\right)_{small\,\eta} = \left(\frac{RT}{i_o F\left(\alpha_a + \alpha_c\right) A_e}\right) = \left(\frac{RT}{2 i_o n F \theta_{eff} \beta_o A_e}\right)$$

Intrinsic Charge Transfer Resistance (based on θ_{eff} =1 reference condition, full surface availability for charge transfer):

$$R_{ct,o} = \left(\frac{RT}{i_o F\left(\alpha_{a,o} + \alpha_{c,o}\right) A_e}\right) = \left(\frac{RT}{2 i_o n F \beta_o A_e}\right)$$
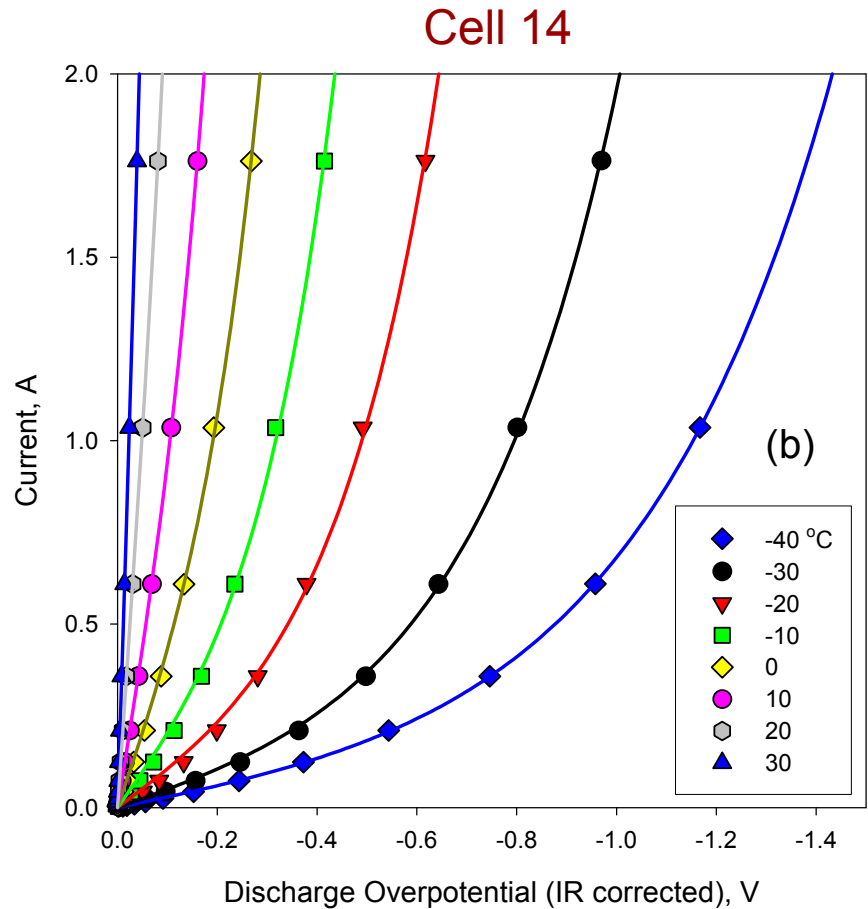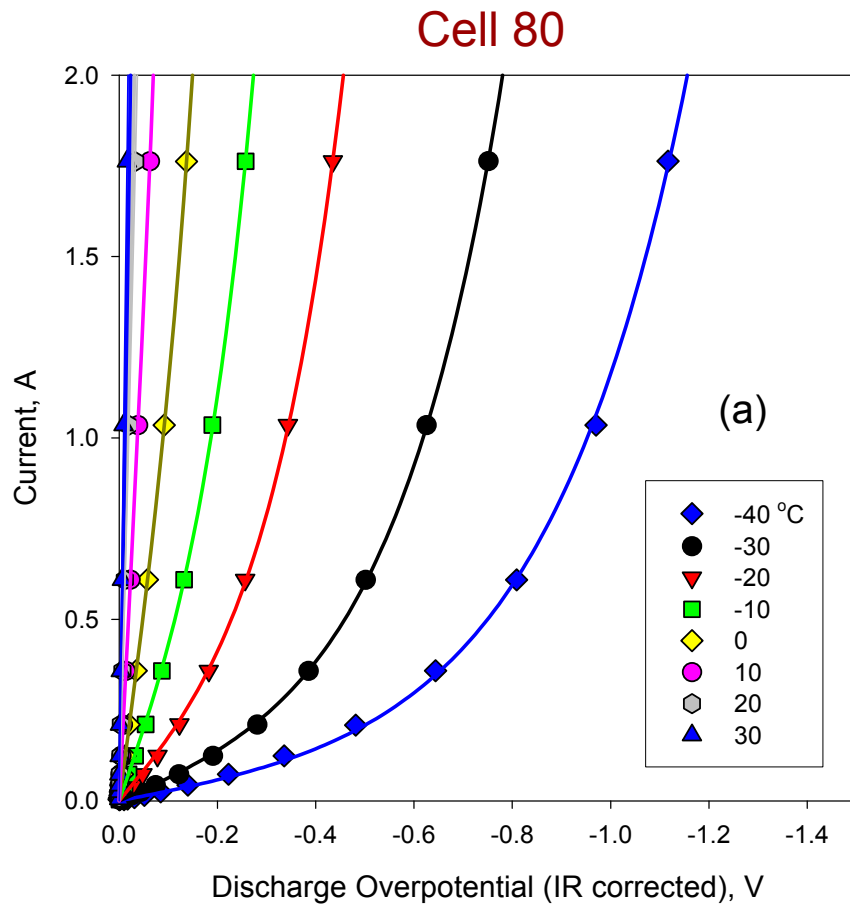
Charge Transfer Resistance attributed to transport limitations at critical interfacial regions of electrodes:

$$R_{int} = (R_{ct,app} - R_{ct,o}) = \left(\frac{RT}{2 i_o n F \beta_o A_e}\right)\left(\frac{1}{\theta_{eff}} - 1\right)$$

Thus, $\quad \theta_{eff} = \dfrac{R_{ct,o}}{R_{int} + R_{ct,o}} \quad \Big| \quad R_{total} = R_{ct,app} + R_{ohm} = R_{int} + R_{ct,o} + R_{ohm}$

(applicable to short pulses)

Example of θ-BV Model Results

Cell 80

(a)

Cell 14

(b)

Current, A

Discharge Overpotential (IR corrected), V

Legend:
- -40 °C
- -30
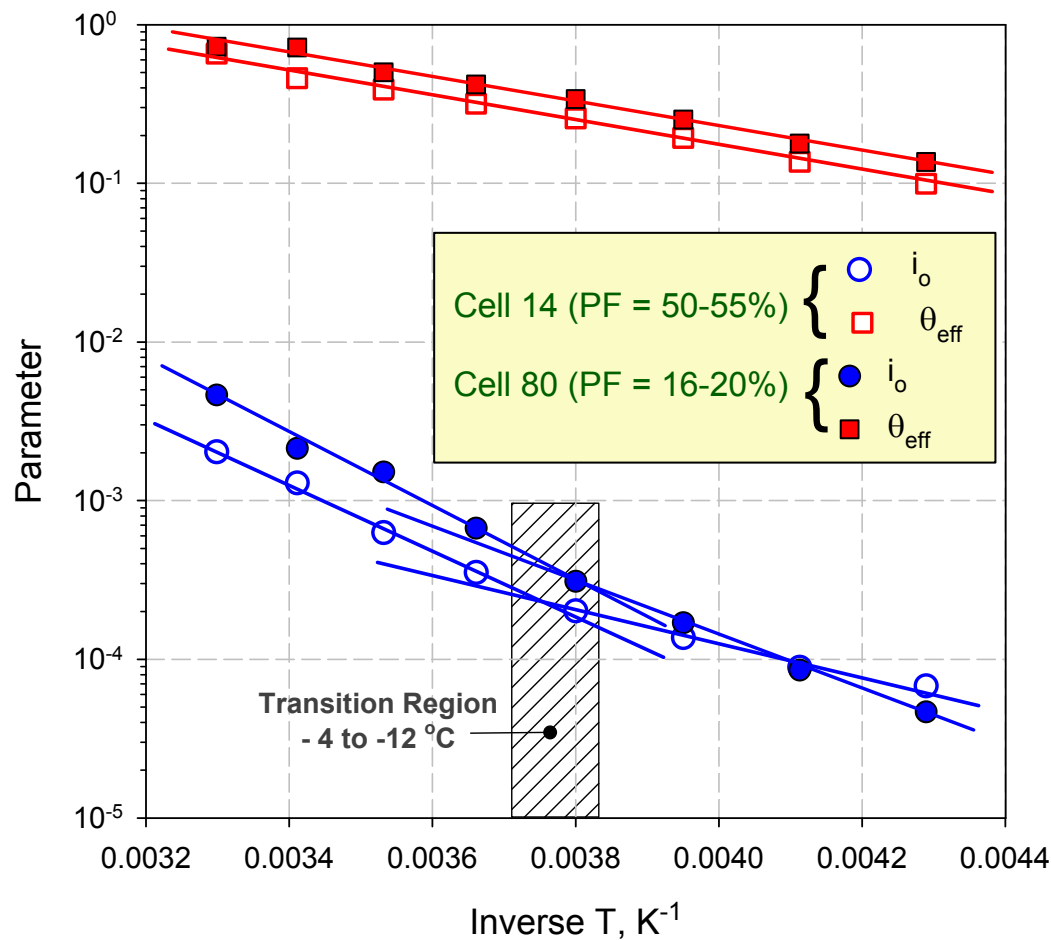- -20
- -10
- 0
- 10
- 20
- 30

Symbols: from constant-current pulse data (4-s)

Solid Curves: from θ-BV regression
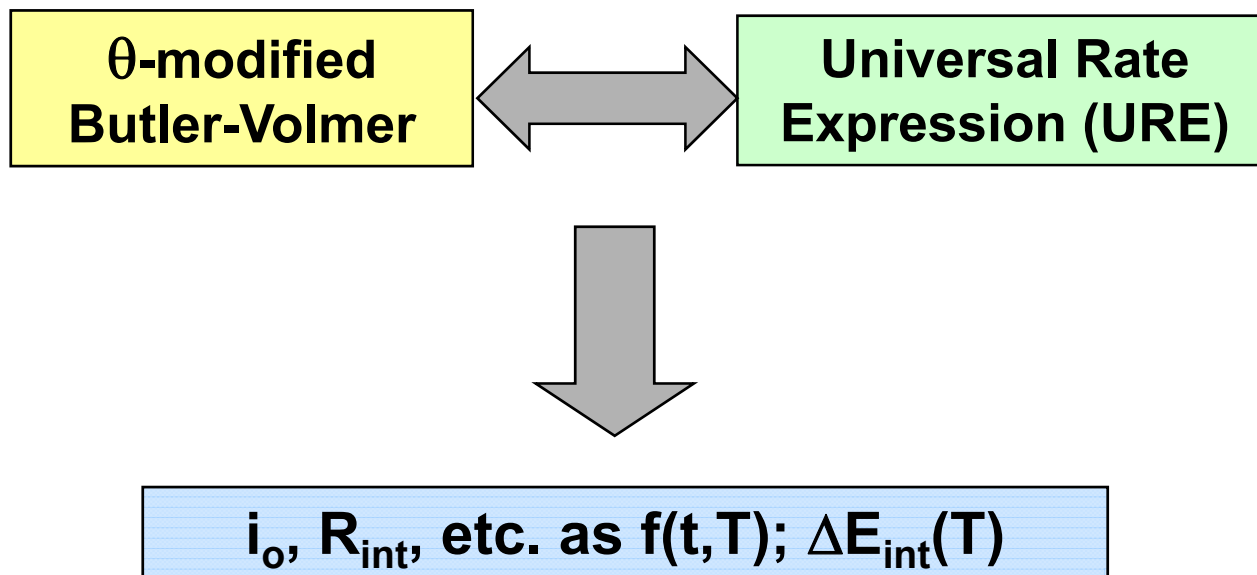
$R^2 \geq 0.999$ in all cases

Example of θ-BV Model Parameters (assessed at 4s pulse)

Both θ_{eff} and i_o decrease at lower temperatures, indicating constrained interfacial transport and greater electrochemical irreversibility.

Generalizing θ-BV Model to (t,T) Domains

Since it is desirable to *predict* cell behavior during a pulse, the θ-BV is trained by URE to render accurate prediction over (t,T):

θ-modified Butler-Volmer $\longleftrightarrow$ Universal Rate Expression (URE)

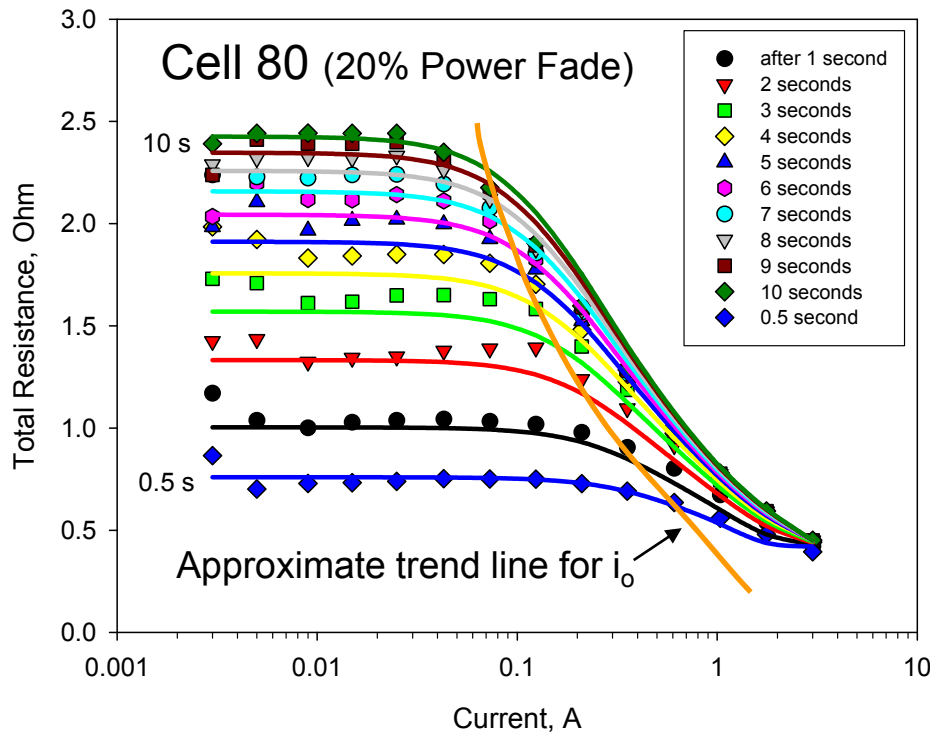i_o, R_{int}, etc. as f(t,T); $\Delta E_{int}(T)$

$\rightarrow$ a powerful predictive capability for low temperature performance

Results over (t,T) Domains (discharge)

Model results (solid curves) show impressive accuracy for (t,T) conditions
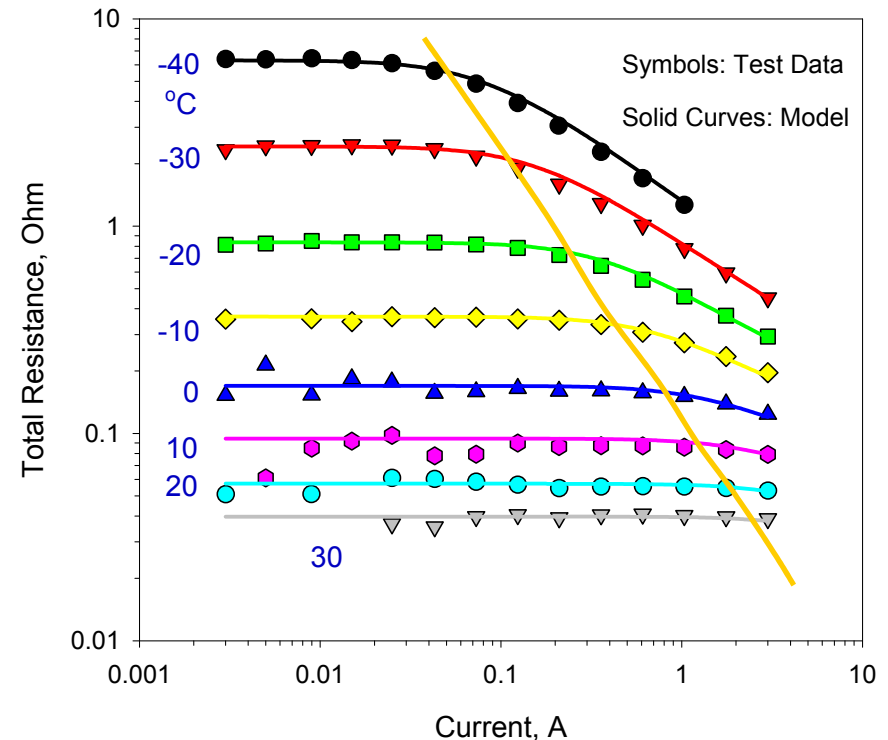

R_{total} at –30 °C along pulse timeline

R_{total} at 10 s over temperature

The exchange current density (i_o) decreases over elapsed pulse time.
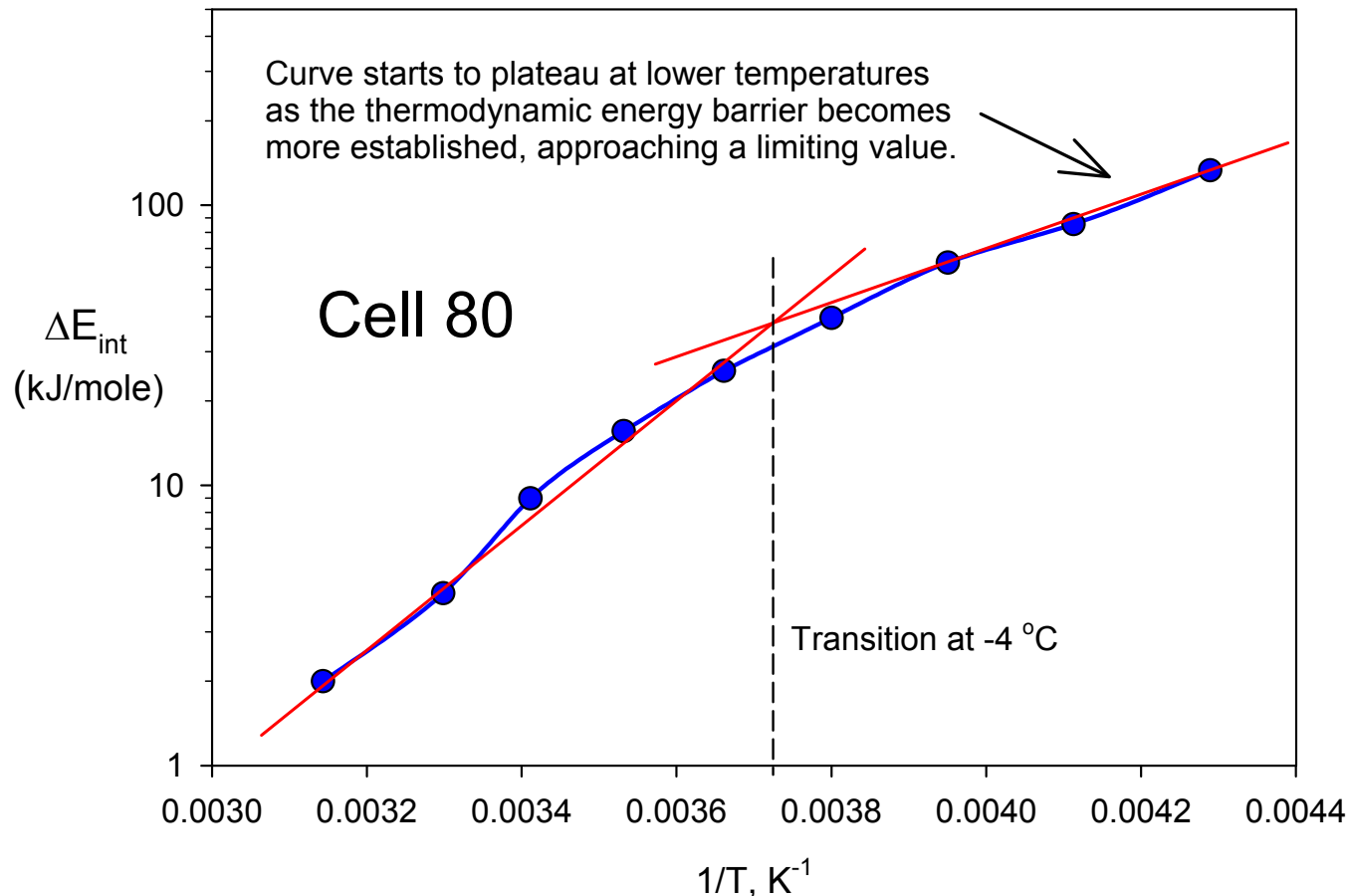
R_{total} starts to plateau by the end of pulse.

i_o decreases with decreasing temperature.

Data scatter at higher T is due to extremely small voltage drops (sub-mV).

Interfacial Energy Barrier

This plot quantifies the interfacial energy barrier that is encountered within the cell while discharging. ΔE_{int} is obtained from analysis of isothermal impedance profiles in concert with θ-BV/URE.

Curve starts to plateau at lower temperatures as the thermodynamic energy barrier becomes more established, approaching a limiting value.

Cell 80

ΔE_{int} (kJ/mole)
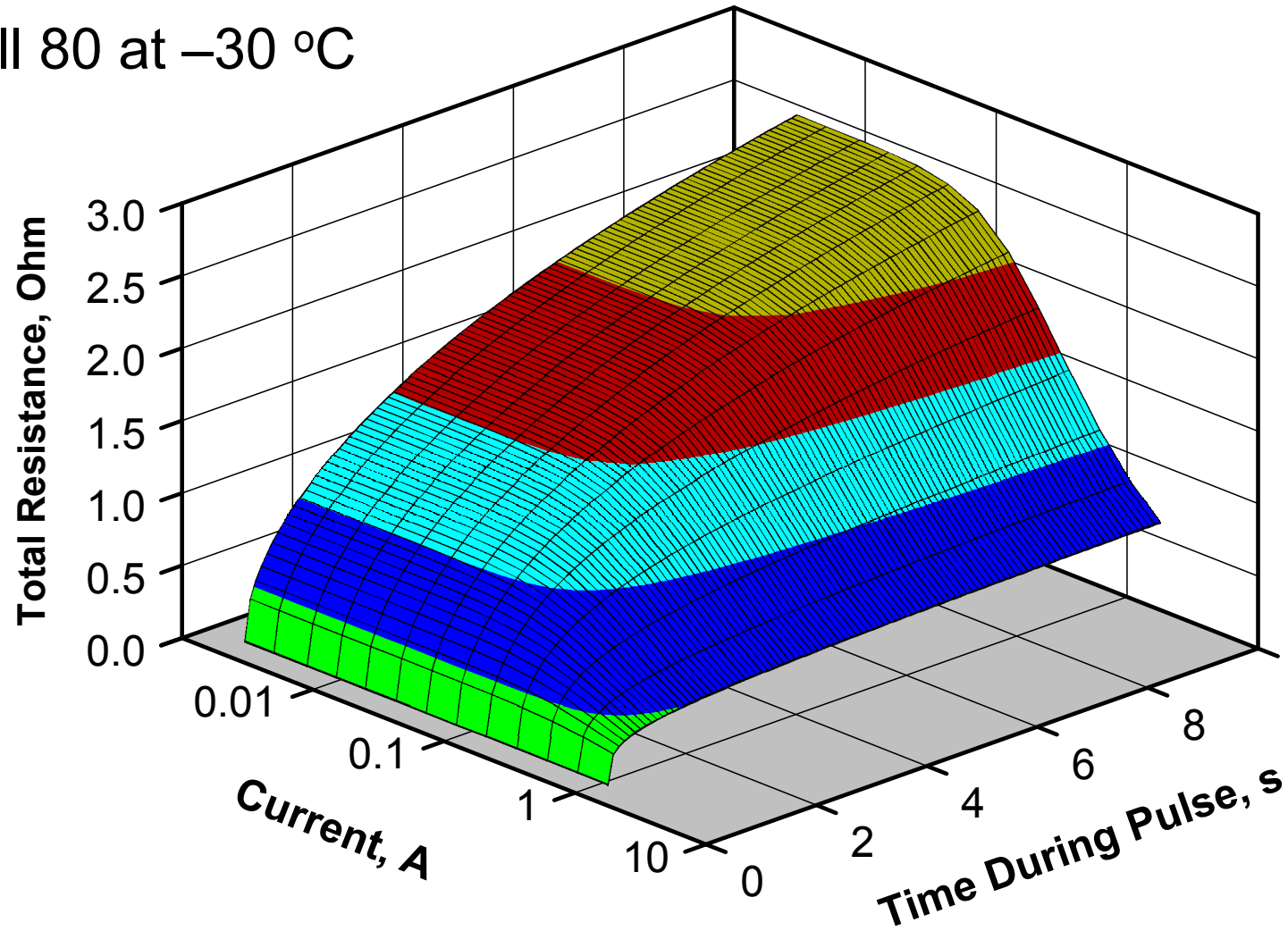
Transition at -4 ^{o}C

1/T, K^{-1}

These results infer one or more *thermodynamic processes* occur over temperature to increase the interfacial impedance.

Mechanisms for this could include increased solvent ordering, rearrangement, adsorption, or phase formation at electrode interfaces and inside porous regions, *which are more prone to occur at OCV conditions*.
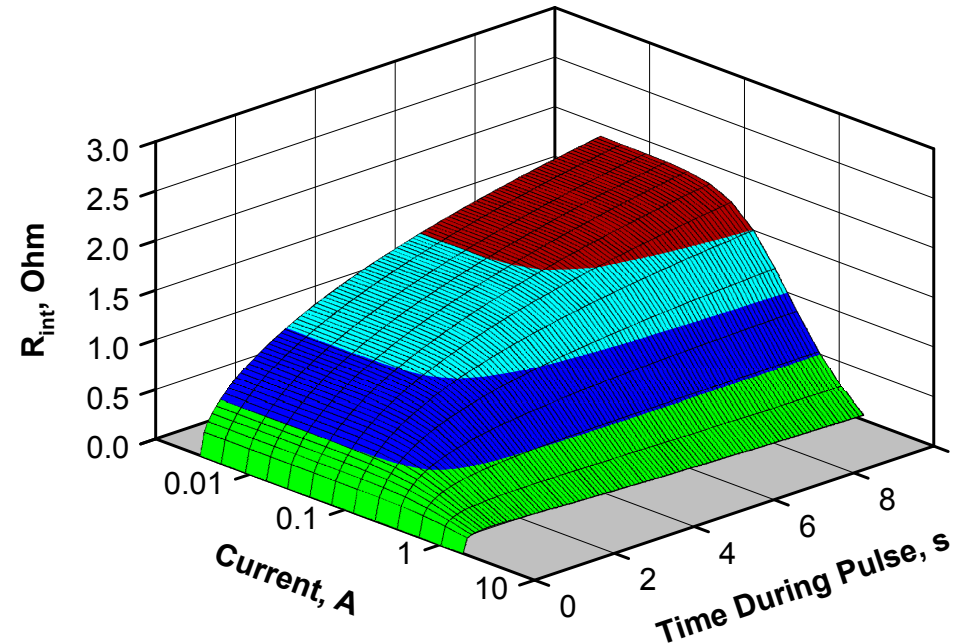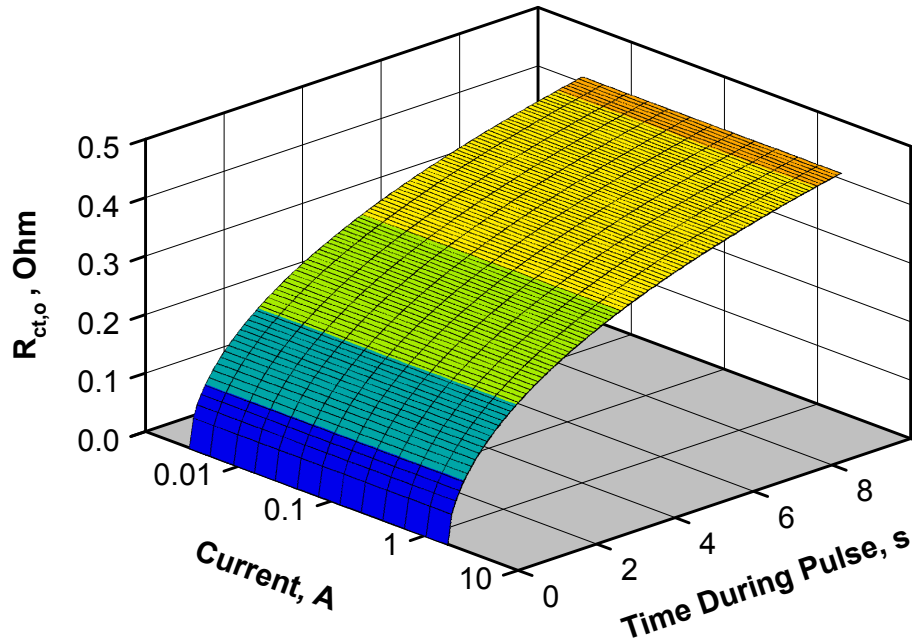
Predicted 3D Profile: R$_{total}$

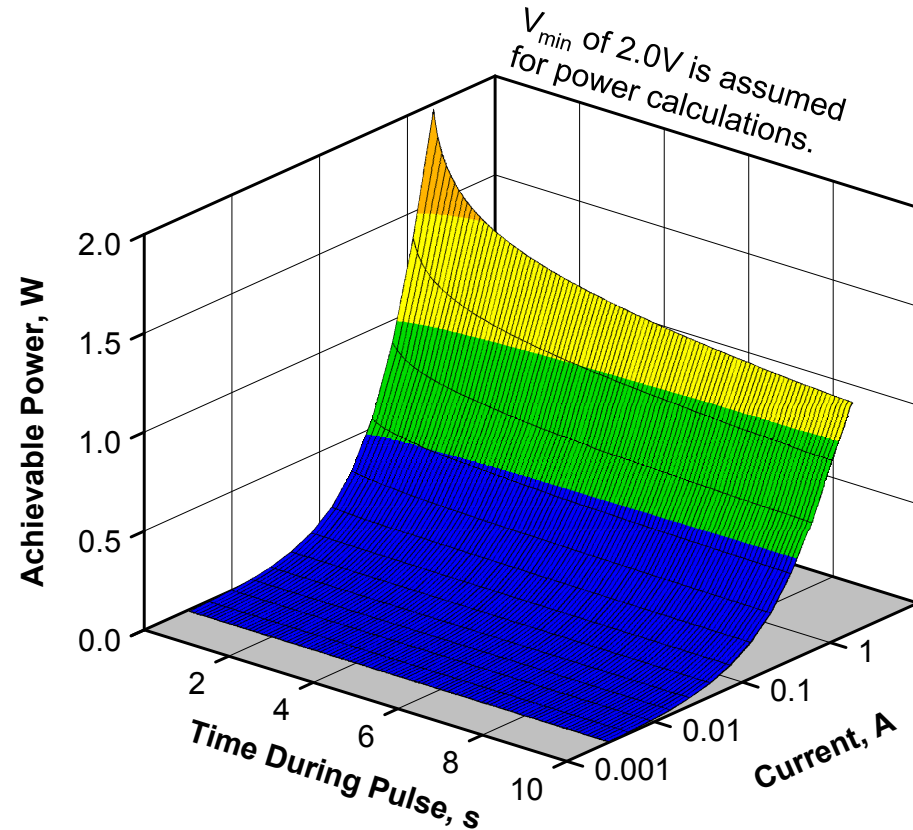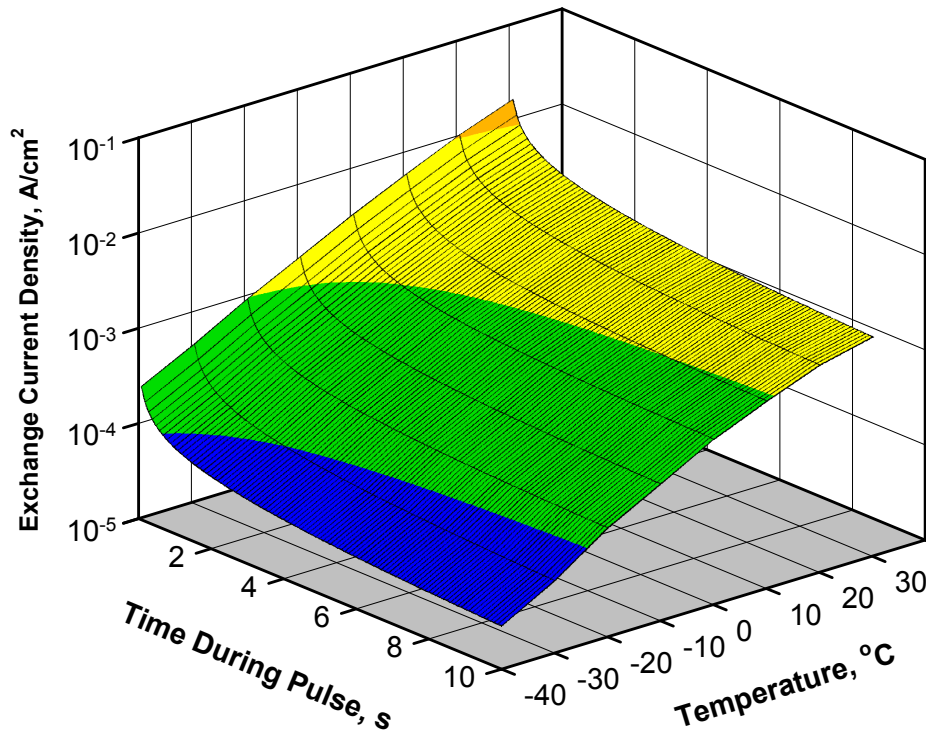Cell 80 at –30 ^{o}C

Predicted 3D Profiles: $R_{ct, o}$ and R_{int}

Cell 80 at $-30\ ^oC$

- ❐ Note the difference in scale: $R_{ct, o} < R_{int}$
- ❐ $R_{ct, o}$ is constant over current for a given t since i_o is not variant over current for isothermal systems ($R_{ct, o} = RT/(2\beta_o i_o nFA_e)$). $R_{ct, o}$ can drop at high currents if there is sufficient joule heating.

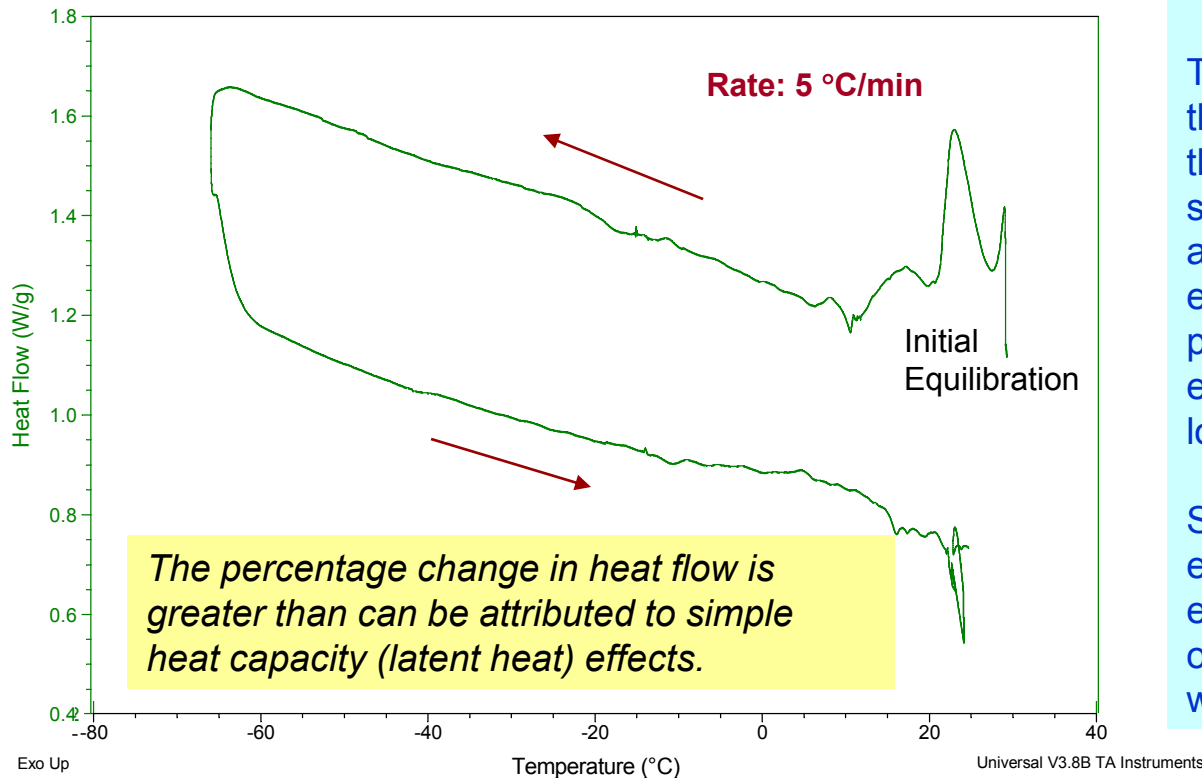# Predicted 3D Profiles: i_o and $P_{achiev.}$

Cell 80 at –30 °C

Such predictions over t_{pulse}, I, T, and cell aging make for a powerful diagnostic tool and development aid.

Other Supporting Data and Plausible Mechanisms that Address Data Trends

Idaho National Laboratory

DSC Study of Li-ion Cell Materials

Sample DSC results for placing Gen2 electrolyte
with harvested Gen2 electrode materials

Rate: 5 °C/min
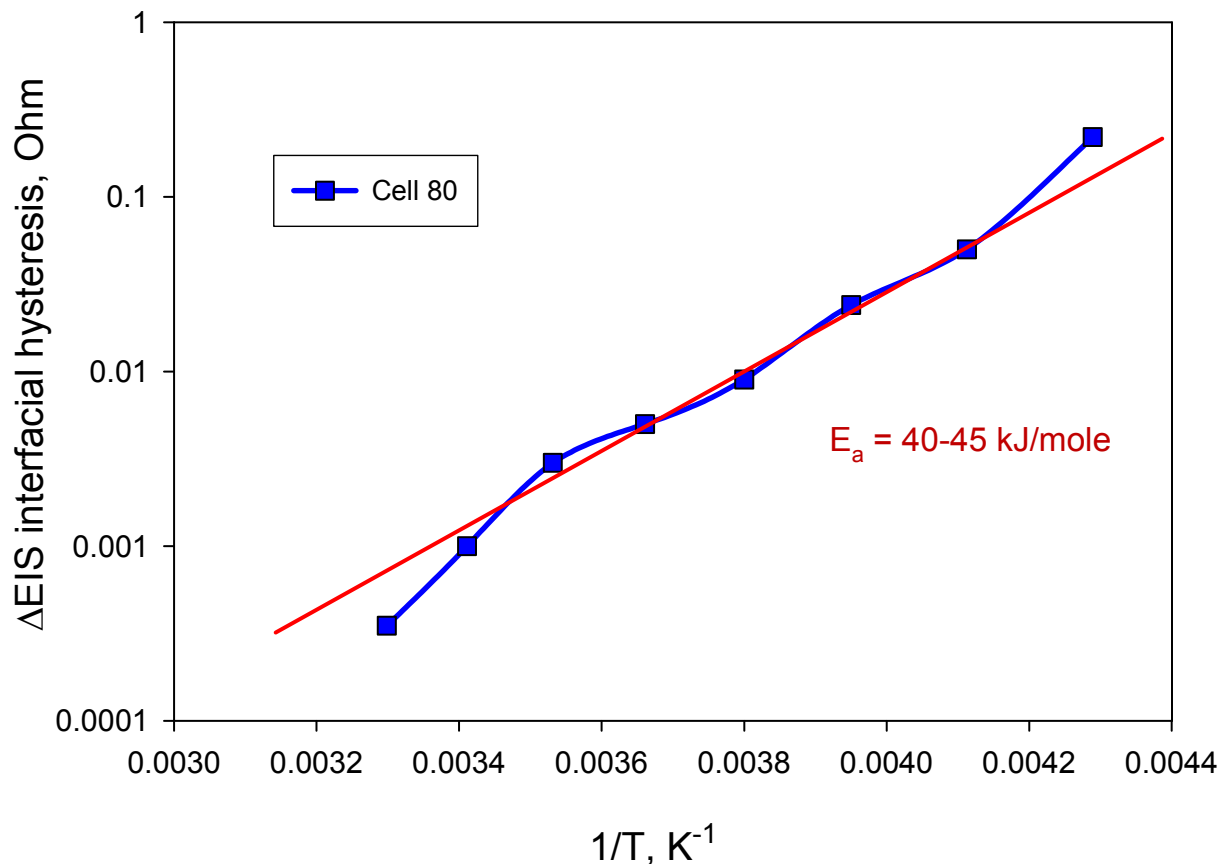
Initial
Equilibration

*The percentage change in heat flow is
greater than can be attributed to simple
heat capacity (latent heat) effects.*

Exo Up

Universal V3.8B TA Instruments

Note that the near-linear trend
over T is similar to linearity of θ_{eff}
from the θ-BV model.

These results infer there are
thermodynamic contributions to
the observed heat flow: perhaps
solvent ordering, rearrangement,
adsorption, or self-association at
electrode interfaces and inside
porous regions to a greater
extent as the temperature is
lowered.

Such mechanisms could help
explain the high activation
energy tied to SEI films, as
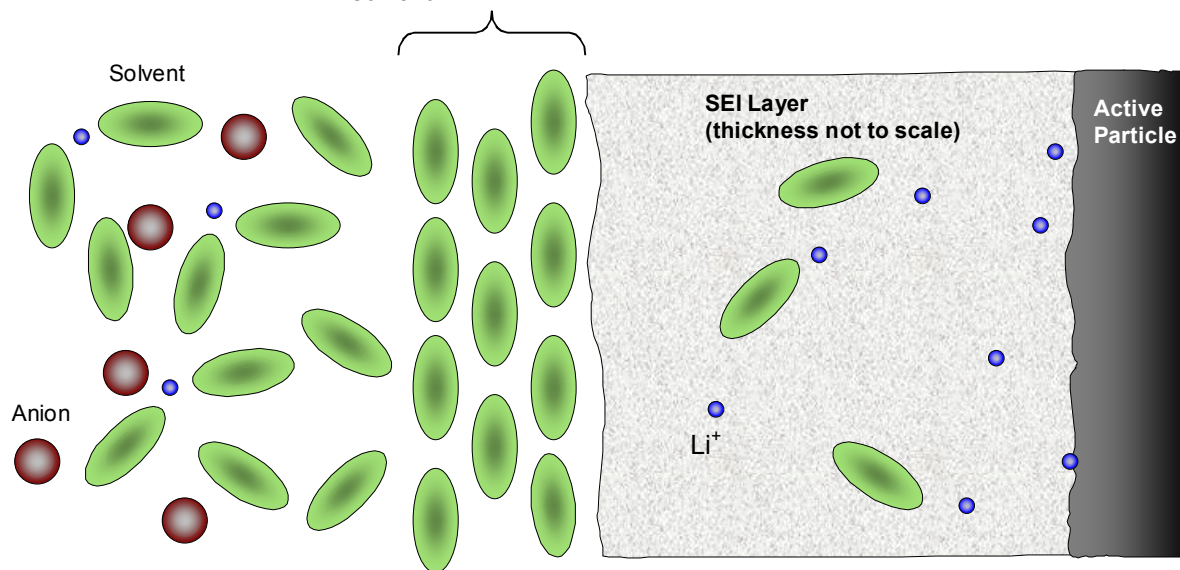observed in EIS semi-circle
widths over temperature.

Hysteresis within semicircle region of moderately aged Gen2 18650 cell, showing the difference in impedance between heating and cooling legs.

E_a = 40-45 kJ/mole

Cell was taken through cooling then heating, and allowed to reach thermal equilibrium between EIS measurements.

These results infer some form of *thermodynamic process* occurs over time to increase the impedance of successive EIS measurements (e.g., increased solvent ordering, rearrangement, adsorption, or phase formation at electrode interfaces and inside porous regions).
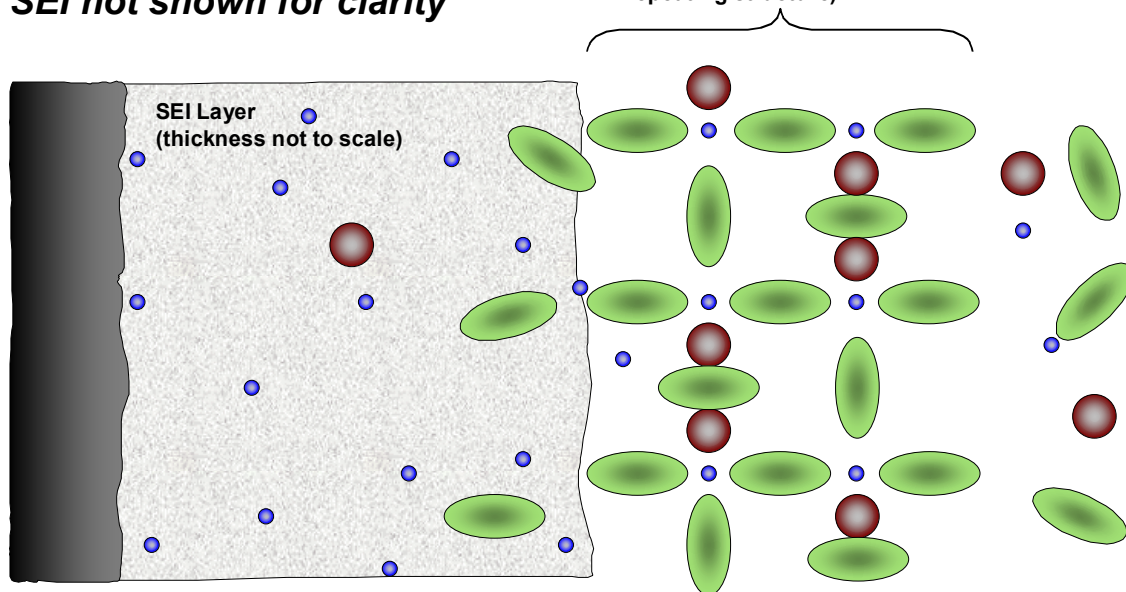
SEI Surface provides local region of reduced energy for structured rearrangement of solvent.

Solvent

Anion

SEI Layer (thickness not to scale)

Active Particle

Li⁺

Examples of surface-promoted phase behavior of electrolyte in Li-ion cells (e.g., Gibbs Adsorption at low T); some more prone to occur at OCV where such thermodynamic processes can ensue.
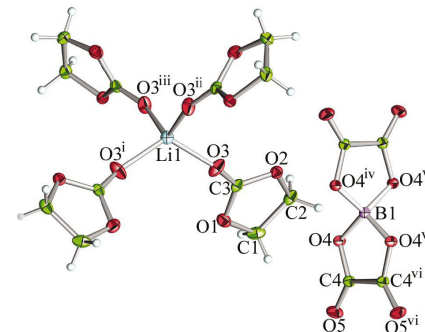
Surface and porous structure of SEI not shown for clarity

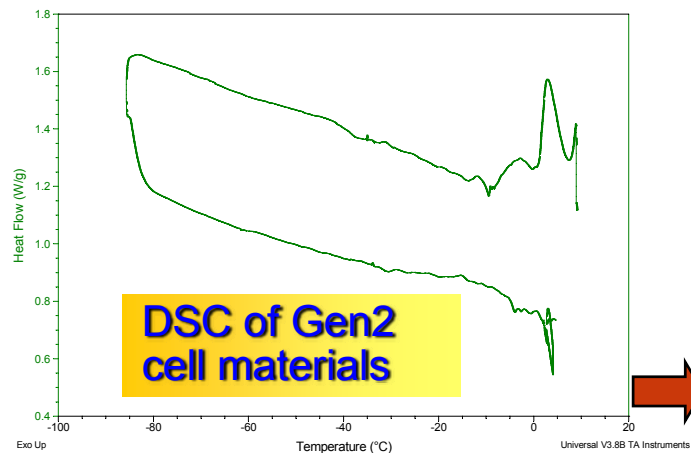Surface-promoted formation of solid solvate (a 2D example of repeating structure)

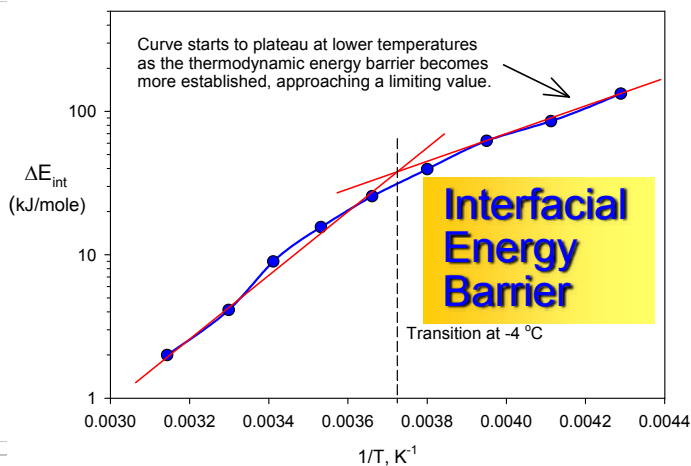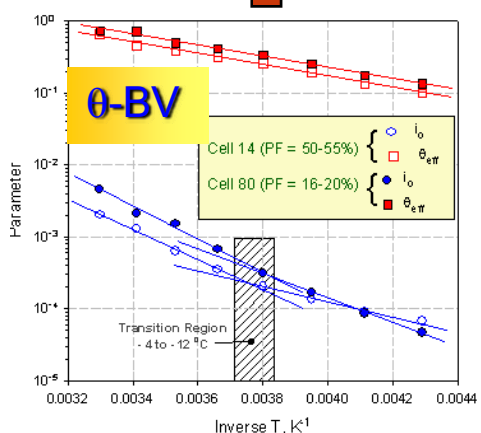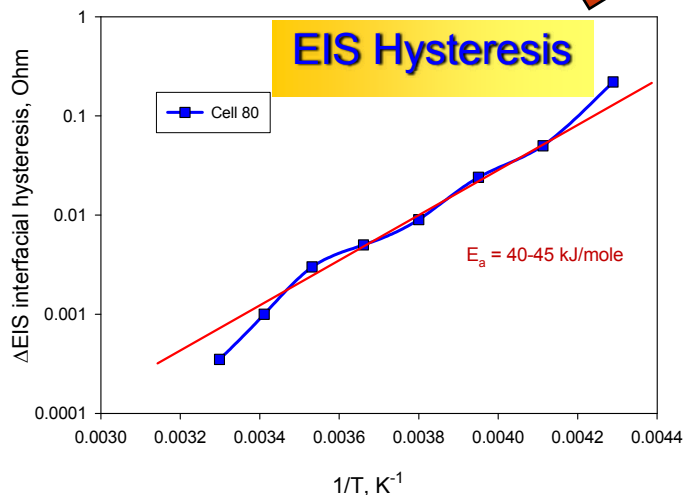SEI Layer (thickness not to scale)

Solvate based on LiBOB(EC)$_4$

S. Whittingham (also Zavalij et al., Acta Cryst., Vol. B60, 716-724 (2004).)

Independent testing and modeling all point to probable thermodynamic mechanisms behind poor performance at low temperatures.

DSC of Gen2 cell materials

EIS Hysteresis
E_a = 40-45 kJ/mole
Cell 80
ΔEIS interfacial hysteresis, Ohm
1/T, K^{-1}

These results infer one or more *thermodynamic processes* occur to increase SEI interfacial impedance at lower temperatures, perhaps by increased solvent ordering, rearrangement, adsorption, or phase formation at electrode interfaces and inside porous regions.

θ-BV
Cell 14 (PF = 50-55%) { i_o, θ_{eff} }
Cell 80 (PF = 16-20%) { i_o, θ_{eff} }
Transition Region - 4 to - 12 °C
Parameter
Inverse T, K^{-1}

Pulse Studies
after 1 second
2 seconds
3 seconds
4 seconds
5 seconds
6 seconds
7 seconds
8 seconds
9 seconds
10 seconds
0.5 second
Total Resistance, Ohm
Current, A

Interfacial Energy Barrier
Curve starts to plateau at lower temperatures as the thermodynamic energy barrier becomes more established, approaching a limiting value.
ΔE_{int} (kJ/mole)
Transition at -4 °C
1/T, K^{-1}

Summary / Conclusions

❒ Transport calculations revealed increased trends of spatial variance of electrolyte composition and properties within DL regions at lower temperatures. While these results are informative and novel, these effects cannot fully account for observed limitations in low temperature performance.

❒ Constant-current pulse studies were performed with Gen2 18650 cells covering a large matrix of charge and discharge currents and temperatures. Data analysis produced a new form of the Butler-Volmer expression (θ-BV) that accounts for the effective electrode surface availability for the charge transfer process. The resultant kinetics model was extended to produce excellent predictions of cell impedance over temperature, current, and pulse-time.

❒ **This work and ancillary lab studies support the conclusion that low temperature performance of Li-ion cells is dominated by an interfacial energy barrier that is likely based on thermodynamic behavior of the electrolyte solvent at interfacial regions.** Interfacial processes that impact the overall charge transfer efficiency (rate) will cause impedance to rise, and collectively, these attributes contribute to large voltage drops and power loss at low temperatures.

> Therefore, mitigation of poor performance at low temperatures must involve:
>
> 1. surface/chemical modification of SEI films to diminish solvent attraction,
>
> 2. thin, compact SEI films that will allow more effective solvent management under pulse conditions.
>
> *SEI Formation Studies are an essential aspect of improved cell performance!*

Future Work

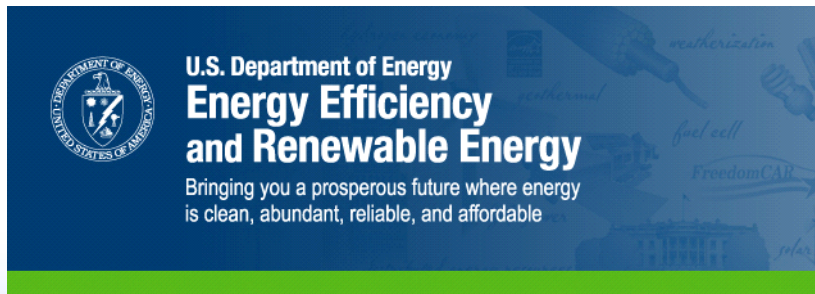**For Low-temperature Performance subtask completion:**

- Perform θ-BV analysis on charge pulse data already obtained at the INL, and compare to analysis of discharge data.

Other Modeling Support (ongoing):

- Investigate the role of structure, porosity, surface charge density, and other attributes of interfacial regions as they pertain to dynamic electrolyte-interface interactions, considering molecular-scale interactions where feasible.

- Model and characterize new or novel candidate electrolytes of interest to DOE-ABRT, and provide results to ABRT participants. This is of abiding interest due to the increased number of new solvents and salts being developed annually.

- Continue to perform diagnostic testing that complements modeling and that will illuminate plausible mechanistic origins of both good and poor performance of Li-ion cells, with emphasis on interfacial processes.

- *There is still a clear need for knowledge regarding mechanistic origins of interface-driven limitations in Li-ion cells at all temperatures. By virtue, this must involve molecular-level investigations.*

Idaho National Laboratory

Acknowledgements

- David Howell, DOE-EERE

- Vehicle Technologies Program

- Dennis Dees, ANL

- David Jamison, INL

- Tim Murphy, INL

- Sergiy Sazhin, INL

U.S. Department of Energy
Energy Efficiency and Renewable Energy
Bringing you a prosperous future where energy is clean, abundant, reliable, and affordable

This work was performed for the United States Department of Energy under contract DE-AC07-05ID14517.

Idaho National Laboratory